ФІЗИКА І ХІМІЯ ТВЕРДОГО ТІЛА
Т. 8, № 3 (2007) С. 494-499

PHYSICS AND CHEMISTRY OF SOLID STATE
V. 8, № 3 (2007) P. 494-499

PACS 66.30.JT, 66.30.LW, 85.40.RY

ISSN1729-4428

F.F .Komarov[1], A.F. Komarov[1], A.M. Mironov[1], G.M. Zayats[2], V.A. Tsurko[2], O.I. Velichko[3]

Simulation of Rapid Thermal Annealing of Low-Energy Implanted Arsenic in Silicon

[1]Institute of Applied Physics Problems of the Belarusian State University,
7 Kurchatov Street, 220064 Minsk, E-mail: KomarovF@bsu.by
[2]Institute of Mathematics, Belarusian Academy of Sciences,
11 Surganov Street, 220072 Minsk, Belarus. E-mail: vtsurko@im.bas-net.by
[3]Belarusian State University of Computer Science and Radioelectronics,
6 P.Brovka Street, 220013 Minsk, Belarus. E-mail: oleg_velichko@lycos.com

Two-dimensional model of As thermal diffusion is presented. The model was developed taking into consideration nonlinearity of the process, cluster formation, influence of point defects. For the calculation of the impurity distribution profile at rapid thermal annealing, an efficient numerical algorithm based on a finite-difference method was applied. Results of calculations are compared to experimental data.

Key words: Numerical simulation, diffusion and ion implantation technology, defects, impurities, silicon

Стаття поступила до редакції 07.01.2007; прийнята до друку 15.06.2007.

Introduction

Low-energy ion implantation is widely used for the formation of active areas in modern integrated microcircuits elements. The combination of low-energy (1–30 keV) ion implantation and rapid thermal annealing allows fabricating devices with ultra-shallow junctions [1–4]. Such technologies of impurity doping lead to the formation of impurity profiles of a complex shape [5, 6]. The modelling of such processes is impossible without application of physical and mathematical description with a high degree of adequacy as well as involving effective numerical methods. Application of the commonly used process simulators like ATHENA SSUPREM4 of SILVACO not always provides satisfactory accurate results. In a surface region of the semiconductor (1–50 nm depth), the impurity distribution profiles calculated using such software can essentially differ from experimental results [5, 6]. At the same time, the exact information on dopant distribution in proximity of the surface is necessary for effective calculation of the electric characteristics of modern semiconductor devices.

In the present work, the two-dimensional model of thermal diffusion of arsenic in silicon is developed on the basis of our researches [7–9]. In our model, the migration of implanted arsenic is described in view of nonlinearity of the process, influence of point defects, cluster formation and migration of electrons. In contrast to the known models of arsenic diffusion in silicon, we consider that clusterization depends not only on a level of the impurity concentration, but also on concentration of electrons. Such approach allows to model precisely enough distribution of the impurity at a surface of semiconductor crystal at low-energy implantation and rapid thermal annealing.

For the numerical solution of the constructed nonlinear systems of differential equations, the method of final differences [10, 11] is used. We developed the economic locally-one-dimensional schemes [11] allowing to model the diffusion in two dimensions quickly enough. Results of some numerical calculations, in comparison with experimental data, are presented.

I. The model

We suggest that arsenic diffusion occurs due to the formation, migration, and dissociation of the “$As^{+}D^{r}$” pairs, where As^{+} and D^{r} are the substitutionally dissolved arsenic atom and intrinsic point defect, respectively [12]. At a construction of the model of point defects evolution we do certain simplifications. We assume that As diffusion occurs substantially by the interstitial mechanism, and diffusion by vacancies is less significant. Therefore we consider only the equation describing diffusion of point defects induced by transfer of intrinsic interstitial atoms. We assume also that the drift of intrinsic interstitial atoms and vacancies in the field of internal elastic stress is negligible. A thermodynamic approach based on the local equilibrium

between the substitutionally dissolved arsenic, point defects and the pairs leads to the following system of diffusion equations:

$$\frac{\partial C^{T}}{\partial t}=\sum_{k=1}^{2}\frac{\partial}{\partial x_k}\left(D(\chi)\left(\frac{\partial}{\partial x_k}(\tilde{C}C)+\frac{\tilde{C}C}{\chi}\frac{\partial\chi}{\partial x_k}\right)\right), \quad (1)$$

$$\sum_{k=1}^{2}\frac{\partial^2\tilde{C}}{\partial x_k^2}-\frac{\tilde{C}}{l_i^{\times 2}}+\frac{\tilde{C}^{g}}{l_i^{\times 2}}=0, \quad (2)$$

where (1) is the equation of dopant atoms diffusion and (2) is the equation of diffusion of point defects [9];

$$C^{T}=C+C^{AC}, \qquad \tilde{C}=C^{\times}/C_i^{\times}, \qquad D_i=D_i^{\times}+D_i^{1}+D_i^{2},$$

$$D^{C}(\chi)=\frac{1+\beta_1\chi+\beta_2\chi^2}{1+\beta_1+\beta_2}, \; \beta_j=\frac{D_i^{j}}{D_i^{\times}}, \; j=1,2,$$

where C and C^{AC} are the concentrations of substitutionally dissolved arsenic atoms and dopant atoms incorporated into clusters, respectively; $D = D(\chi)$ and D_i are the effective and intrinsic diffusivities of arsenic, respectively; $D_i^{\times}$ D_i^{1}, and D_i^{2} are the partial diffusion coefficients due to interactions of the dopant atoms with the neutral, singly, and doubly charged defects, respectively; χ is the concentration of electrons normalized to the intrinsic carrier concentration n_e; $C^{\times}$ is the concentration of point defects in the neutral charge state; $C_i^{\times}$ is the equilibrium concentration of neutral point defects in the bulk of the semiconductor, $l_i^{\times}$ is the average migration length of point defects; $\tilde{C}^{g}$ is the effective generation rate of point defects normalized to the rate of equilibrium thermal generation:

$$\tilde{C}^{g}=1+g(x_1,x_2)/g_i,$$

where g_i is the total defect generation rate in different charge states in an intrinsic semiconductor; the function $g(x_1, x_2)$ in the case of $l_i^{\times}\geq\Delta y^{d}$ and $l_i^{\times}\geq\Delta R_p^{d}$ can be approached by the following analytical expression [13]:

$$g(x_1,x_2)=\frac{G(x_1)}{2}\left[\operatorname{erf}\left(\frac{x_2+a}{\sqrt{2}\Delta y^{d}}\right)-\operatorname{erf}\left(\frac{x_2-a}{\sqrt{2}\Delta y^{d}}\right)\right].$$

Here

$$G(x_1)=\frac{p^{d}}{\sqrt{2\pi}\Delta R_p^{d}}\exp\left[\frac{(x_1-R_p^{d})^2}{2(\Delta R_p^{d})^2}\right],$$

where p^d is the defect generation power at arsenic ion implantation, R_p^{d} is the position of maximum of generated defects distribution, ΔR_p^{d} is the depth dispersion, Δy^{d} is the lateral deviation of the generated defects. The concentration of clustered arsenic atoms can be obtained from the following expression [9]:

$$C^{AC}=K\tilde{C}_D\chi^4C^2,$$

where K is the characteristic parameter of clustering; $\tilde{C}_D$ is the normalized concentration of the defects participating in the cluster formation. We used the $K\tilde{C}_D$ value of 3.0×10^{-16} μm³ at a temperature of 950 °C. The parameter value has been taken from [9]. To calculate values of χ, a condition of local charge neutrality was used:

$$\chi=n/n_e=\frac{C-C^{AC}-C^{B}+\sqrt{(C-C^{AC}-C^{B})^2+4n_e^2}}{2n_e}, \quad (3)$$

where C^B is the summarized concentration of acceptors.

The simulation domain is considered as a flat cut of a masked silicon substrate transversely to the surface (Fig. 1): $G=\{0\leq x_1\leq l_1, 0\leq x_2\leq l_2\}$ is a rectangle with sides l_1 and l_2, A is the border of simulation area: $A = A_1 + A_2 + A_3 + A_4$, $2a$ is the width of not-masked surface.

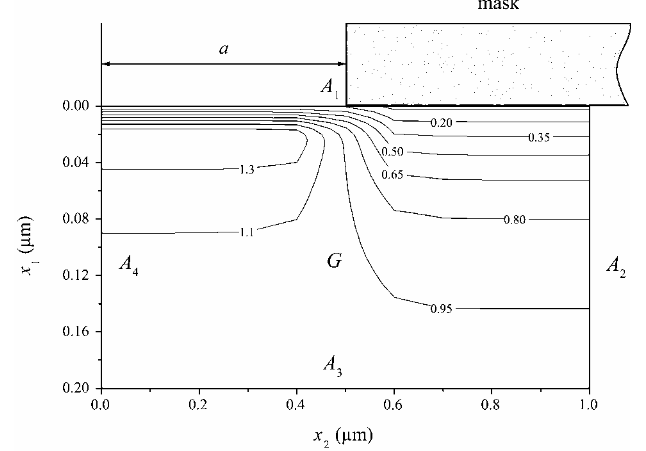

Fig. 1. The simulation domain and the normalised two-dimensional distribution of point defects.

For the Equation (1) on the boundary A let us consider the following condition:

$$D(\chi)\left(\frac{\partial\tilde{C}C}{\partial\mathbf{n}}+\frac{\tilde{C}C}{\chi}\frac{\partial\chi}{\partial\mathbf{n}}\right)=0, \quad (4)$$

where **n** is the normal vector to the simulation boundary.

The initial conditions are following

$$C^{T}(x_1,x_2,t)\big|_{t=0}=C_0(x_1,x_2), \quad (5)$$

where $C_0(x_1, x_2)$ is the distribution of the implanted atoms.

Equation (2) is closed by the conditions:

$$\tilde{C}\big|_{A_1}=\alpha(x_2),$$

$$\text{where } \alpha(x_2)=\begin{cases}\alpha-\text{const}<1, & \text{if } 0\leq x_2\leq a,\\ \beta, & \text{if } a<x_2\leq l_2\end{cases}$$

$$\tilde{C}\big|_{A_2}=1,\; \tilde{C}\big|_{A_3}=1,\; \frac{\partial\tilde{C}}{\partial x_2}\bigg|_{A_4}=0. \quad (6)$$

In case of a mask, for example, from silicon nitride, $\beta = 0$.

II. Numerical method

For the purpose of calculation acceleration, it is possible to use domains of different size for As atoms and point defects diffusion modelling. The values of l_1 and l_2 for the solution of Eq. (2) should be large enough to guarantee correctness of the boundary conditions $\tilde{C}\big|_{A_2}=1$ and $\tilde{C}\big|_{A_3}=1$. At the same time, the

problem of the modelling of low-energy implanted dopant is solved, as a rule, in much smaller area. Therefore, it is enough to take the defects distribution corresponding to the area of modelling of As diffusion (Eq.(1)) with the purpose of reduction of the calculation time.

Let us introduce a non-uniform time grid:

$$\omega_\tau = \left\{ t_0 = 0,\ t_j = \sum_{k=1}^{j} \tau_k,\ j = 1,2,...,j_0, \tau_k > 0 \right\}.$$

The calculation grid on spatial variables ω_h has the following form:

$$\omega_h = \{0 \le x_{1,i_1} \le l_1,\ 0 \le x_2, i_2 \le l_2,\ x_{1,0} = x_{2,0} = 0,$$
$$x_{1,i_1} = x_{1,0} + i_1 h_1, i_1 = \overline{1, N_1},\quad x_{2,i_2} = x_{2,0} + i_2 h_2, i_2 = \overline{1, N_2}\}.$$

For the effective solution of the Equation (1) we used a locally-one-dimensional method [11]. Let us put a chain of the one-dimensional equations in correspondence with the Eq. (1):

$$\frac{\partial C^T_{(1)}}{\partial t} = \frac{\partial}{\partial x_1}\left(D(\chi_{(1)}) \left(\frac{\partial(\tilde{C}C_{(1)})}{\partial x_1} + \frac{\tilde{C}C_{(1)}}{\chi_{(1)}} \frac{\partial \chi_{(1)}}{\partial x_1} \right) \right), \tag{7}$$

$t_{j-1} \le t \le t_j,\quad (x_1, x_2) \in G,$

$$\frac{\partial C^T_{(2)}}{\partial t} = \frac{\partial}{\partial x_2}\left(D(\chi_{(2)}) \left(\frac{\partial(\tilde{C}C_{(2)})}{\partial x_2} + \frac{\tilde{C}C_{(2)}}{\chi_{(2)}} \frac{\partial \chi_{(2)}}{\partial x_2} \right) \right), \tag{8}$$

$t_{j-1} \le t \le t_j,\quad (x_1, x_2) \in G.$

The equations (7) and (8) are connected by the conditions

$$C_{(1)}\big|_{t=t_{j-1}} = C_{(2)}\big|_{t=t_{j-1}}, j = 2,3,...,j_0,$$
$$C_{(2)}\big|_{t=t_{j-1}} = C_{(1)}\big|_{t=t_j}, j = 1,2,...,j_0, C^T_{(1)}\big|_{t=0} = C_0(x_1, x_2).$$

The values of $\chi_{(1)}$ and $\chi_{(2)}$ are defined from (3); $C^T_{(m)} = C_{(m)} + \tilde{K}\chi^4_{(m)} C^2_{(m)}$, where $\tilde{K} = K\tilde{C}_D$.

Boundary conditions for the Equations (7) and (8) are the following:

$$D(\chi_{(1)}) \left(\frac{\partial(\tilde{C}C_{(1)})}{\partial x_1} + \frac{\tilde{C}C_{(1)}}{\chi_{(1)}} \frac{\partial \chi_{(1)}}{\partial x_1} \right) = 0, \tag{9}$$

$t_{j-1} \le t \le t_j, (x_1, x_2) \in A_\nu, \nu = 1,3$

$$D(\chi_{(2)}) \left(\frac{\partial(\tilde{C}C_{(2)})}{\partial x_2} + \frac{\tilde{C}C_{(2)}}{\chi_{(2)}} \frac{\partial \chi_{(2)}}{\partial x_2} \right) = 0, \tag{10}$$

$t_{j-1} \le t \le t_j, (x_1, x_2) \in A_\nu, \nu = 2,4.$

One-dimensional problems (7), (9) and (8), (10) are solved along the lines $x_2 = x_{2,i_2}, i_2 = 0,1,...,N_2$ and the lines $x_1 = x_{1,i_1}, i_1 = 0,1,...,N_1$, respectively.

According to the theory of a locally-one-dimensional method [11], we assume that the functions $C_{(2)}$ and $C^T_{(2)}$ are the approximate solution of the problem (1)–(6) at the time moment $t = t_j, j = 1,2,...,j_0$.

Let $y^T_{(m)}, y_{(m)}, z_{(m)}, \tilde{y}$, $m = 1,2$, are the grid functions defined on the grid $\omega = \omega_\tau \times \omega_h$ and let they correspond to the functions $C^T_{(m)}$, $C_{(m)}$, $\chi_{(m)}$, $\tilde{C}$, $m = 1,2$.

The symbols introduced here for difference relations are the same as in [11].

Using the integrointerpolation method [11], we will construct the nonlinear difference Crank-Nicolson schemes for the differential conditions (7)–(10).

For Eq. (7) on the grid ω at $i_2 = 0,1,2,...,N_2$ we have the following difference equations:

$$\left(y^T_{(1)}(z_{(1)}, y_{(1)})\right)_{\bar{\tau}}\Big|^j_{i_1} = \frac{1}{2}\left(\left(a_1(z_{(1)})\bar{y}_{(1)\bar{x}_1} + \bar{a}_1(z_{(1)}, \bar{y}_{(1)}) z_{(1)\bar{x}_1}\right)_{x_1}\right)\Big|^j_{i_1} +$$
$$+\frac{1}{2}\left(\left(a_1(z_{(1)})\bar{y}_{(1)\bar{x}_1} + \bar{a}_1(z_{(1)}, \bar{y}_{(1)}) z_{(1)\bar{x}_1}\right)_{x_1}\right)\Big|^{j-1}_{i_1}, \tag{11}$$

$i_1 = 1,...,N_1 - 1,\quad j = 1,2,...,j_0,$

where $\bar{y}_{(1)}\big|_{i_1,i_2} = \left(\tilde{y}\, y_{(1)}\right)\big|_{i_1,i_2},\quad i_1 = 0,1,...,N_1.$

Using the differential equation (7), on the boundary A_1 we approximate the condition (9) by the following relation:

$$0,5h_1\left(y^T_{(1)}(z_{(1)}, y_{(1)})\right)_{\bar{\tau}}\Big|^j_{i_1=0} = \frac{1}{2}(a_1(z_{(1)})\bar{y}_{(1)\bar{x}_1} +$$
$$+\bar{a}_1(z_{(1)}, \bar{y}_{(1)}) z_{(1)\bar{x}_1})\Big|^j_{i_1=1} + \frac{1}{2}(a_1(z_{(1)})\bar{y}_{(1)\bar{x}_1} + \tag{12}$$
$$+\bar{a}_1(z_{(1)}, \bar{y}_{(1)}) z_{(1)\bar{x}_1})\Big|^{j-1}_{i_1=1},\quad j = 1,2,...,j_0.$$

Similarly, on the boundary $x_1 = l_{x_1}$ relation

$$-0,5h_1\left(y^T_{(1)}(z_{(1)}, y_{(1)})\right)_{\bar{\tau}}\Big|^j_{i_1=N_1} = \frac{1}{2}(a_1(z_{(1)})\bar{y}_{(1)\bar{x}_1} +$$
$$+\bar{a}_1(z_{(1)}, \bar{y}_{(1)}) z_{(1)\bar{x}_1})\Big|^j_{i_1=N_1} + \frac{1}{2}(a_1(z_{(1)})\bar{y}_{(1)\bar{x}_1} + \tag{13}$$
$$+\bar{a}_1(z_{(1)}, \bar{y}_{(1)}) z_{(1)\bar{x}_1})\Big|^{j-1}_{i_1=N_1},\quad j = 1,2,...,j_0$$

is obtained.

In Eq. (11)–(13) the grid functions $a_1(z_{(1)})$ and $\bar{a}_1(z_{(1)}, \bar{y}_{(1)})$ are defined as follows:

$$a_1\left(z_{(1)}\right) = 0,5\left(D\left(z_{(1)}\left(x_{i_1}, x_{i_2}, t_j\right)\right) + D\left(z_{(1)}\left(x_{i_1-1}, x_{i_2}, t_j\right)\right)\right),$$
$$\bar{a}_1\left(z_{(1)}, \bar{y}_{(1)}\right) = 0,5\left(D\left(z_{(1)}\left(x_{i_1}, x_{i_2}, t_j\right)\right) \frac{\bar{y}_{(1)}\left(x_{i_1}, x_{i_2}, t_j\right)}{z_{(1)}\left(x_{i_1}, x_{i_2}, t_j\right)} + \right.$$
$$\left. + D\left(z_{(1)}\left(x_{i_1-1}, x_{i_2}, t_j\right)\right) \frac{\bar{y}_{(1)}\left(x_{i_1-1}, x_{i_2}, t_j\right)}{z_{(1)}\left(x_{i_1-1}, x_{i_2}, t_j\right)} \right),$$

$i_1 = 1,2,...,N_1,\quad i_2 = 0,1,...,N_2,\quad j = 0,1,...,j_0.$

Similarly, the differential equation (8) on the grid ω at $i_1 = 0,1,...,N_1$ is approximated by the difference relations of the form

$$\left(y^{T}_{(2)}(z_{(2)},y_{(2)})\right)_{\bar{t}}\Big|^{j}_{i_2} = \frac{1}{2}\left(\left(a_2(z_{(2)})\bar{y}_{(2)\bar{x}_2}+\bar{a}_2(z_{(2)},\bar{y}_{(2)})z_{(2)\bar{x}_2}\right)_{x_2}\right)\Big|^{j}_{i_2}+\frac{1}{2}\left(\left(a_2(z_{(2)})\bar{y}_{(2)\bar{x}_2}+\bar{a}_2(z_{(2)},\bar{y}_{(2)})z_{(2)\bar{x}_2}\right)_{x_2}\right)\Big|^{j-1}_{i_2}, \quad (14)$$

$i_2 = 1,...,N_2-1, \quad j=1,2,...,j_0.$

Here $\bar{y}_{(2)}\big|_{i_1,i_2} = \left(\tilde{y}y_{(2)}\right)\big|_{i_1,i_2}, \quad i_2 = 0,1,...,N_2.$

For the boundary condition (10) on the boundary line A_2 we construct the difference approximation

$$0,5h_2\left(y^{T}_{(2)}(z_{(2)},y_{(2)})\right)_{\bar{t}}\Big|^{j}_{i_2=0} = \frac{1}{2}(a_2(z_{(2)})\bar{y}_{(2)\bar{x}_2}+\bar{a}_2(z_{(2)},\bar{y}_{(2)})z_{(2)\bar{x}_2})\Big|^{j}_{i_2=1}+\frac{1}{2}(a_2(z_{(2)})\bar{y}_{(2)\bar{x}_2}+\bar{a}_2(z_{(2)},\bar{y}_{(2)})z_{(2)\bar{x}_2})\Big|^{j-1}_{i_2=1}, \quad j=1,2,...,j_0. \quad (15)$$

Similarly, for $(x_1,x_2)\in A_4$ we obtain the following difference relations

$$-0,5h_2\left(y^{T}_{(2)}(z_{(2)},y_{(2)})\right)_{\bar{t}}\Big|^{j}_{i_2=N_2} = \frac{1}{2}(a_2(z_{(2)})\bar{y}_{(2)\bar{x}_2}+\bar{a}_2(z_{(2)},\bar{y}_{(2)})z_{(2)\bar{x}_2})\Big|^{j}_{i_2=N_2}+\frac{1}{2}(a_2(z_{(2)})\bar{y}_{(2)\bar{x}_2}+\bar{a}_2(z_{(2)},\bar{y}_{(2)})z_{(2)\bar{x}_2})\Big|^{j-1}_{i_2=N_2}, \quad j=1,2,...,j_0. \quad (16)$$

In the relations (14)–(16) the grid functions $a_2(z_{(2)})$ and $\bar{a}_2(z_{(2)},\bar{y}_{(2)})$ are defined as follows:

$$a_2\left(z_{(2)}\right) = 0,5\left(D\left(z_{(2)}\left(x_{i_1},x_{i_2},t_j\right)\right)+D\left(z_{(2)}\left(x_{i_1},x_{i_2-1},t_j\right)\right)\right),$$

$$\bar{a}_2\left(z_{(2)},\bar{y}_{(2)}\right) = 0,5\left(D\left(z_{(2)}\left(x_{i_1},x_{i_2},t_j\right)\right)\frac{\bar{y}_{(2)}\left(x_{i_1},x_{i_2},t_j\right)}{z_{(2)}\left(x_{i_1},x_{i_2},t_j\right)}+,\ +D\left(z_{(2)}\left(x_{i_1},x_{i_2-1},t_j\right)\right)\frac{\bar{y}_{(2)}\left(x_{i_1},x_{i_2-1},t_j\right)}{z_{(2)}\left(x_{i_1},x_{i_2-1},t_j\right)}\right)$$

$i_1 = 0,1,...,N_1, \quad i_2 = 1,2,..,N_2, \quad j=0,1,...,j_0.$

Problems (11)–(13) and (14)–(16) are connected by the following conditions

$$y_{(1)}\big|_{t=t_{j-1}} = y_{(2)}\big|_{t=t_{j-1}},\ y_{(2)}\big|_{t=t_{j-1}} = y_{(1)}\big|_{t=t_j},\ y^{T}_{(1)}\big|_{t=0} = C_0(x_1,x_2).$$

We complete the system of the difference relations (11)–(13), (14)–(16) and (17) by algebraic nonlinear equations

$$z_{(m)}-\frac{1}{2n_e}\left(y_{(m)}-\tilde{K}z^4_{(m)}y^2_{(m)}-C_B+\sqrt{\left(y_{(m)}-\tilde{K}z^4_{(m)}y^2_{(m)}-C_B\right)^2+4n_e^2}\right)\Big|^{j}_{i_1,i_2}=0, \quad (17)$$

where

$m=1,2; \quad j=0,1,...,j_0; \quad i_1=0,1,...,N_1; \quad i_2=0,1,...,N_2.$

We construct the initial conditions for the difference problem (11)–(13) using the relations (3) and (5):

$$\begin{cases} y_{(1)}+\tilde{K}z^4_{(1)}y^2_{(1)} = C_0\big|_{i_1,i_2}, \\ z_{(1)}-\frac{1}{2n_e}\left(y_{(1)}-\tilde{K}z^4_{(1)}y^2_{(1)}-C_B+\sqrt{\left(y_{(1)}-\tilde{K}z^4_{(1)}y^2_{(1)}-C_B\right)^2+4n_e^2}\right)\Big|_{i_1,i_2}=0, \end{cases} \quad (18)$$

where $i_1 = 0,1,..,N_1,\ i_2=0,1,..,N_2.$

Approximate solution of the algebraic equations system (18) is obtained by the method of interval bisection.

On the grid ω_h the equation (2) is approximated by the following system of the difference relations:

$$\left(\sum_{k=1}^{2}\tilde{y}_{\bar{x}_k x_k}-\frac{\tilde{y}}{l_i^{\times 2}}+\frac{\tilde{C}^g}{l_i^{\times 2}}\right)\Bigg|_{i_1,i_2}=0, \quad (19)$$

$i_1 = 1,2,...,N_1-1; \quad i_2 = 1,2,...,N_2-1.$

The difference equations (19) jointly with the corresponding boundary conditions are solved by the block-Thomas algorithm [14].

The difference relations (11)–(19) are the closed system of the nonlinear algebraic equations for every $j=1,2,...,j_0$. We find the solution of this system using the same iterative processes.

For the nonlinear equation (11) at $i_2 = 0,1,...,N_2$ we construct the following iterative process

$$\left(y^{T}_{(1)}\left(\overset{s}{z}_{(1)}\overset{s}{y}_{(1)}\right)+\left(1+2\overset{s}{\gamma}_{(1)}\overset{s}{y}_{(1)}\right)\left(\overset{s+1}{y}_{(1)}-\overset{s}{y}_{(1)}\right)\right)\Big|^{j}_{i_1} = y^{T}_{(1)}\left(z_{(1)}y_{(1)}\right)\Big|^{j-1}_{i_1}+\frac{\tau_j}{2}\left(\left(a_1(\overset{s}{z}_{(1)})\tilde{y}\overset{s+1}{y}_{(1)\bar{x}_1}+\bar{a}_{(1)}(\overset{s}{z}_{(1)},\overset{s}{y}_{(1)})\overset{s}{z}_{(1)\bar{x}_1}\right)_{x_1}\right)\Big|^{j}_{i_1}+\frac{\tau_j}{2}\left(\left(a_1(z_{(1)})\bar{y}_{(1)\bar{x}_1}+\bar{a}_{(1)}(z_{(1)},y_{(1)})z_{(1)\bar{x}_1}\right)_{x_1}\right)\Big|^{j-1}_{i_1}. \quad (20)$$

Here $\overset{s}{\gamma}_{(1)} = K\overset{s}{z}{}^4_{(1)}, \quad \overset{s}{\bar{y}}_{(1)} = \tilde{y}\overset{s}{y}_{(1)};$

$i_1 = 1,2,...,N_1-1; \quad s=0,1,2,....$

For the boundary conditions (12) and (13) we have, respectively

$$\xi_j\left(y^{T}_{(1)}\left(\overset{s}{z}_{(1)}\overset{s}{y}_{(1)}\right)+\left(1+2\overset{s}{\gamma}_{(1)}\overset{s}{y}_{(1)}\right)\left(\overset{s+1}{y}_{(1)}-\overset{s}{y}_{(1)}\right)\right)\Big|^{j}_{i_1=0} = \xi_j\,y^{T}_{(1)}\left(z_{(1)}y_{(1)}\right)\Big|^{j-1}_{i_1=0}+\frac{1}{2}\left(a_1(\overset{s}{z}_{(1)})\tilde{y}\overset{s+1}{y}_{(1)\bar{x}_1}+\bar{a}_1(\overset{s}{z}_{(1)},\overset{s}{\bar{y}}_{(1)})\overset{s}{z}_{(1)\bar{x}_1}\right)^{j}_{i_1=1}+\frac{1}{2}\left(a_1(z_{(1)})\bar{y}_{(1)\bar{x}_1}+\bar{a}_1(z_{(1)},\bar{y}_{(1)})z_{(1)\bar{x}_1}\right)^{j-1}_{i_1=1}; \quad (21)$$

-

$$\xi_j\left(y^{T}_{(1)}\left(\overset{s}{z}_{(1)}\overset{s}{y}_{(1)}\right)+\left(1+2\overset{s}{\gamma}_{(1)}\overset{s}{y}_{(1)}\right)\left(\overset{s+1}{y}_{(1)}-\overset{s}{y}_{(1)}\right)\right)\Big|^{j}_{i_1=N_1} = -\xi_j\,y^{T}_{(1)}\left(z_{(1)}y_{(1)}\right)\Big|^{j-1}_{i_1=N_1}++\frac{1}{2}\left(a_1(\overset{s}{z}_{(1)})\tilde{y}\overset{s+1}{y}_{(1)\bar{x}_1}+\bar{a}_1(\overset{s}{z}_{(1)},\overset{s}{\bar{y}}_{(1)})\overset{s}{z}_{(1)\bar{x}_1}\right)^{j}_{i_1=N_1}+\frac{1}{2}\left(a_1(z_{(1)})\bar{y}_{(1)\bar{x}_1}+\bar{a}_1(z_{(1)},\bar{y}_{(1)})z_{(1)\bar{x}_1}\right)^{j-1}_{i_1=N_1}, \quad (22)$$

where $\xi_j = 0.5h_1/\tau_j,\ s=0,1,2,....$

The solution of the problem (20)–(22) is obtained by the Thomas algorithm [11]. By analogy with the relations (20)–(22) we construct the iterative procedures for the

solution of the nonlinear equations (14)–(16). For the equation (17) we obtain the following iterative relation

$$\overset{s+1}{z}_{(m)} - \frac{1}{2n_e}\times\left.\left(\overset{s+1}{y}_{(m)} - K\,\overset{s+1}{z}{}^4_{(m)}\,\overset{s+1}{y}{}^2_{(m)} - C_B + \sqrt{\left(\overset{s+1}{y}_{(m)} - K\,\overset{s+1}{z}{}^4_{(m)}\,\overset{s+1}{y}{}^2_{(m)} - C_B\right)^2 + 4n_e^2}\right)\right|^{j}_{i_1,i_2} = 0,$$

$$m = 1,2,\quad j = 0,1,\ldots,j_0,\quad i_1 = 0,1,\ldots,N_1,\quad i_2 = 0,1,\ldots,N_2,\quad s = 0,1,2,\ldots$$

The values of the grid functions $\overset{s+1}{z}_{(m)}, m = 1,2, s = 0,1,2,\ldots,$ on the grid ω taking into account $\overset{s+1}{y}_{(m)}$ is calculated by the method of interval bisection.

The iterations are stopped when

$$\left|\overset{s+1}{y}_{(1)i_1,i_2} - \overset{s}{y}_{(1)i_1,i_2}\right| \le \varepsilon\left|\overset{s}{y}_{(1)i_1,i_2}\right|,\quad i_1 = 0,1,\ldots,N_1,$$

$$i_2 = 0,1,\ldots,N_2,\quad s = 1,2,\ldots,$$

where ε is empirical parameter.

We assume that the numerical solution $y_{(2)}$ is an approximate solution of the problem (1)–(6) at every time layer.

Control of the calculations is realized by the testing of the condition

$$\iint_G y^T_{(2)}(x_1,x_2,t^j)dx_1dx_2 = \iint_G C_0(x_1,x_2)dx_1dx_2\,,$$

$$j = 1,2,\ldots,j_0\,,$$

where $y^T_{(2)} = y_{(2)} + Kz^4_{(2)}y^2_{(2)}$.

III. Results of simulation

We simulated the experiment described in [5]: 10^{15} cm^{-2} 15 keV As^+ ions were implanted at room temperature into Si wafers with (100) orientation and p-type resistivity of 2.5–5.2 Ω·cm. After the ion implantation, the wafers were annealed in a tungsten-halogen lamp system in nitrogen ambient at a temperature of 950 °C for 10 s. The arsenic concentration profile after annealing was measured by ToF-SIMS. The concentration scale for As has been determined using known calibration standard implantations in Si (absolute error 10%), and the depth scale has been determined using ex situ interference microscopy (absolute error < 5%), assuming a constant erosion rate [5].

For the calculation of point defects distribution we used the following values: a = 0,5 μm, α = 0,175, β = 0, $l_i^{\times}$ =0,05 μm, l_1 = 0,4 μm, l_2 = 5 μm. In Fig. 1, the calculated values of the point defects distribution $\tilde{C}$ are presented.

For the simulation of As diffusion we used the following parameters: l_1 = 0,2 μm, l_2 = 1 μm, β_1 = 0,436; β_2 = 0,0; $\tilde{K}$ = $3{,}0\times10^{-16}$ μm^3. In Fig. 2, the two-dimensional profile of As distribution C^T as a result of rapid thermal annealing is presented. In Fig. 3, results of simulation at x_2 = 0 are compared with the experimental data [5].

The calculated profile of the total As concentration agrees well with the experimental data, including the near surface region (Figs. 2, 3). Therefore, the presented model allows simulation of high concentration transient enhanced diffusion of As implanted in Si. The transport process differs substantially from the processes described by the Fick's second law. In our opinion, the non-uniform distribution of point defects plays the main role in the "uphill" diffusion of arsenic atoms near the surface of the semiconductor and formation of local maximum of the dopant concentration. It follows from Eq. (1) that nonuniform distribution of silicon interstitial atoms in the neutral charge state causes the additional flux of impurity atoms, which leads to the "uphill" diffusion. We suppose that radiation induced segregation or matrix effects during SIMS analysis are negligible, because apparent "uphill" diffusion is not observed for the as-implanted As profiles also measured by SIMS.

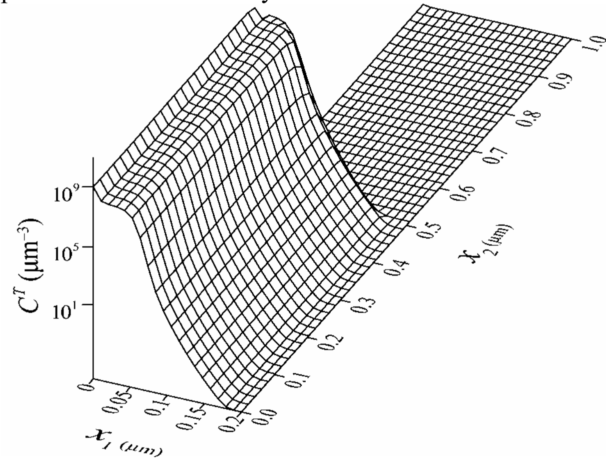

Fig. 2. Simulated two-dimensional As distribution after annealing.

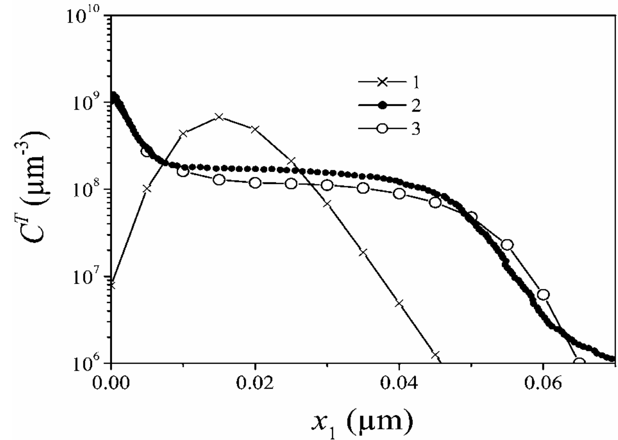

Fig. 3. Simulated As profile before (*1*) and after annealing (*3*) compared to experimental profile (*2*) from [5].

Conclusion

The two-dimensional model of thermal diffusion of arsenic in silicon was developed. We applied the effective difference method of the solving of the constructed system of the differential equations. The offered nonlinear model considers interaction of high

concentration of impurity, point defects and electrons. The model can be used for in modern integrated circuits manufacturing technology for the simulation of rapid thermal annealing. The model predicts the effect of “uphill” diffusion of the implanted arsenic in surface areas of silicon crystal. The simulation results are in a reasonable agreement with experimental data, including the presence of local maximum of the arsenic atoms near the surface.

Комаров Ф.Ф. – д.ф.-м.н., чл.-корр. НАН Беларуси, зав. лаб.;
Комаров А.Ф. – д.ф.-м.н., главный научный сотрудник;
Миронов А.М. – научный сотрудник;
Заяц Г.М. – к.ф.-м.н., старший научный сотрудник;
Цурко В.А. – д.ф.-м.н., главный научный сотрудник;
Величко О.И. – д.ф.-м.н., доцент.

[1] W. Vandervorst, T. Janssens, B. Brijs, T. Conard, C. Huyghebaert, J. Fruhauf, A. Bergmaier, G. Dollinger, T. Buyuklimanli, J.A. VandenBerg, K. Kimura. Errors in near-surface and interfacial profiling of boron and arsenic // *Applied Surface Science*, **231–232**, pp. 618–631 (2004).
[2] T.H. Buyuklimanli, J.W. Marino, S.W. Novak. Improved near surface characterization of shallow arsenic distribution by SIMS depth profiling // *Applied Surface Science*, **231–232**, pp. 636–639 (2004).
[3] L. Ihaddadene-Le Coq, J. Marcon, A. Dush-Nicolini, K. Masmoudi, K. Ketata. Diffusion simulations of boron implanted at low energy (500 eV) in crystalline silicon // *Nuclear Instruments and Methods in Physics Research*, **B216**, pp.303–307 (2004).
[4] F. Boucard, F. Roger, I. Chakarov, V. Zhuk, M. Temkin, X. Montagner, E. Guichard, D. Mathiot. A comprehensive solution for simulating ultra-shallow junctions: From high dose/low energy implant to diffusion annealing // *Materials Science and Engineering* **B124–125**, pp. 409–414 (2005).
[5] D. Girginoudi, N. Georguolas, A. Thanailakis, E.A. Polycroniadis. Studies of ultra shallow n^+-p junctions formed by low-energy As-implantation // *Materials Science and Engineering* **B114–115**, pp. 381–385 (2004).
[6] S. Solmi, M. Ferri, M. Bersani, D. Giubertoni, V. Soncini. Transient enhanced diffusion of arsenic in silicon // *J. Appl. Phys.*, **94**(8), pp. 4950–4955 (2003).
[7] F.F. Komarov, A.M. Mironov, V.A. Tsurko, O.I. Velichko, G.M. Zayats. Modeling of diffusion of As implanted in Si in the near-surface region // *Proceedings of IV International Conference “New Electrical and Electronic Technologies and their Industrial Implementation”, Zakopane, Poland*, pp. 68–70 (2005).
[8] F.F. Komarov, O.I. Velichko, V.A. Dobrushkin, A.M. Mironov. Mechanisms of arsenic clustering in silicon // *Phys. Rew. B*. **74**(3), 035205-1–035205-10 (2006).
[9] F.F. Komarov, O.I. Velichko, A.M. Mironov, V.A. Tsurko, G.M. Zayats. Numerical algorithms for modeling of diffusion of As implanted in Si at low energies and high fluences // *Procedings of SPIE*, **6260**, pp. 566–574 (2006).
[10] R.D. Richtmyer, K.W. Morton. *Difference methods for initial-value problems, Second edition*. Interscience Publishers, New York, 405 p. (1967).
[11] A.A. Samarskii. *Theory of Difference Schemes*. Nauka Publ., Moscow. 656 p. (1977).
[12] O.I. Velichko, A.M. Mironov, V.A. Tsurko, G.M. Zayats. Simulation of arsenic diffusion during rapid thermal annealing of silicon layers doped with low-energy high-dose ion implantation // *Proceedings of IRS, Minsk*, **2**, pp. 197–199 (2005).
[13] H. Ryssel, I. Ruge. *Ion implantation*. Wiley (Chichester and New York), 459 p. (1986).
[14] A.A. Samarskii, E.S. Nikolaev. *Methods for Solving Mesh Equations*. Nauka Publ., Moscow. 592 p. (1978).

Ф.Ф. Комаров[1], А.Ф. Комаров[1], А.М. Миронов[1], Г.М. Заяц[2],
В.А. Цурко[2], О.І. Величко[3]

Моделювання швидкого теплового відпалу низько-енергетичної імплантації миш’яку у кремній

[1]Інститут прикладних проблем фізики Білоруського державного університету, вул. Курчатова, 7, Мінськ, 220064, Біларусь, E-mail: KomarovF@bsu.by
[2]Інститут Математики, Білоруска Академія Наук, вул. Сурганова, 11, Мінськ, 220072, Білорусь, E-mail:vtsurko@im.bas-net.by
[3]Білоруський державний університет інформатики и радіоелектроніки, вул. П. Бровка, Мінськ, 220013, Білорусь, E-mai:l oleg_velichko@lycos.com

Представлена двомірна модель теплової дифузії. Дана модель була запропонована з врахуванням нелінійності процесу, формування кластерів та впливу точкових дефектів. Для розрахунку профілю домішкового розподілу за швидкого термічного відпалу був використаний ефективний числовий алгоритм оснований на методі кінцевої різниці. Результати теоретичних розрахунків близькі до експериментальних даних.